

Contents lists available at ScienceDirect

Fuel

journal homepage: www.elsevier.com/locate/fuel



Full length article

Skeletal reaction models for methane combustion

Yinmin Liu^a, Hessam Babaee^a, Peyman Givi^a, Harsha K. Chelliah^b, Daniel Livescu^c, Arash G. Nouri^{a,*}

- ^a Department of Mechanical Engineering and Materials Science, University of Pittsburgh, Pittsburgh, PA 15261, USA
- ^b Department of Mechanical and Aerospace Engineering, University of Virginia, Charlottesville, VA 22904, USA
- ^c Los Alamos National Laboratory, Los Alamos, NM 87544, USA

ARTICLE INFO

Keywords: Methane-air combustion Skeletal model Local sensitivity analysis Forced optimally time dependent modes High-pressure

ABSTRACT

A local-sensitivity-analysis technique is employed to generate new skeletal reaction models for methane combustion from the foundational fuel chemistry model (FFCM-1). The sensitivities of the thermo-chemical variables with respect to the reaction rates are computed via the forced-optimally time dependent (f-OTD) methodology. In this methodology, the large sensitivity matrix containing all local sensitivities is modeled as a product of two low-rank time-dependent matrices. The evolution equations of these matrices are derived from the governing equations of the system. The modeled sensitivities are computed for the auto-ignition of methane at atmospheric and high pressures with different sets of initial temperatures, and equivalence ratios. These sensitivities are then analyzed to rank the most important (sensitive) species. A series of skeletal models with different number of species and levels of accuracy in reproducing the FFCM-1 results are suggested. The performances of the generated models are compared against FFCM-1 in predicting the ignition delay, the laminar flame speed, and the flame extinction. The results of this comparative assessment suggest the skeletal models with 24 and more species generate the FFCM-1 results with an excellent accuracy.

1. Introduction

There is a continuing need to develop skeletal kinetics models for hydrocarbon combustion [1-3]. These models are typically produced by systematic elimination of unimportant species and reactions from a detailed kinetics model, while maintaining its overall predictive ability [3-6]. Within the past several decades, a variety of techniques have been proposed for this purpose, e.g. local sensitivity analysis (LSA) [7-10], computational singular perturbation [11-13], reaction flux analysis [14-16], and directed relation graph (DRG) and its variants [17-19]. The LSA-based approaches, which are computationally costly for large kinetics models, contain techniques such as principal component analysis [20-26] and species ranking construction [27]. In LSA, the sensitivities can be computed either by solving a sensitivity equation (SE) or by solving an adjoint equation (AE). The latter can become quite costly for time-dependent sensitivity problems, since the AE must be solved in a forward-backward workflow requiring significant I/O costs for large chemical kinetic systems.

The f-OTD method is an on-the-fly reduced order modeling (ROM) technique, recently introduced for computing sensitivities in evolutionary dynamical systems [32]. Unlike, the traditional ROM techniques,

the f-OTD does not require any offline data generation, and all the computations are carried out online. Ref. [10] introduces a LSA-based skeletal kinetics reduction technique that benefits from the computational advantages of the f-OTD, and automatically eliminates unimportant reactions and species. In this approach, the sensitivity matrix i.e. $S(t) \in$ $\mathbb{R}^{n_{eq} \times n_r}$ is approximated by the product of two skinny matrices U(t) = $[u_1(t), u_2(t), \dots, u_r(t)] \in \mathbb{R}^{n_{eq} \times r}$, and $Y(t) = [y_1(t), y_2(t), \dots, y_r(t)] \in \mathbb{R}^{n_r \times r}$ which contain the f-OTD modes and f-OTD coefficients, respectively; with n_{eq} denoting the number of equations (or outputs), n_r the number of independent parameters, $r \ll \min\{n_{eq}, n_r\}$ the reduction size, and $S(t) \approx U(t)Y^{T}(t)$. As shown in [33], the f-OTD type decomposition is an equivalent decomposition to the dynamical low-rank approximation [34]. The computed sensitivities are then analyzed locally to find and rank the most important (sensitive) species. Skeletal models are generated by selecting sufficient number of high ranked species in order to make accurate predictions of physical quantities of interest.

The objective of the present work is to generate accurate skeletal models for methane combustion at atmospheric and high pressure conditions. The f-OTD method is used for modeling local sensitivities of the temperature and the mass fractions with respect to reaction rates, and skeletal reduction is conducted by analyzing these sensitivities and

E-mail address: arash.nouri@pitt.edu (A.G. Nouri).

Corresponding author.

Y. Liu et al. Fuel 357 (2024) 129581

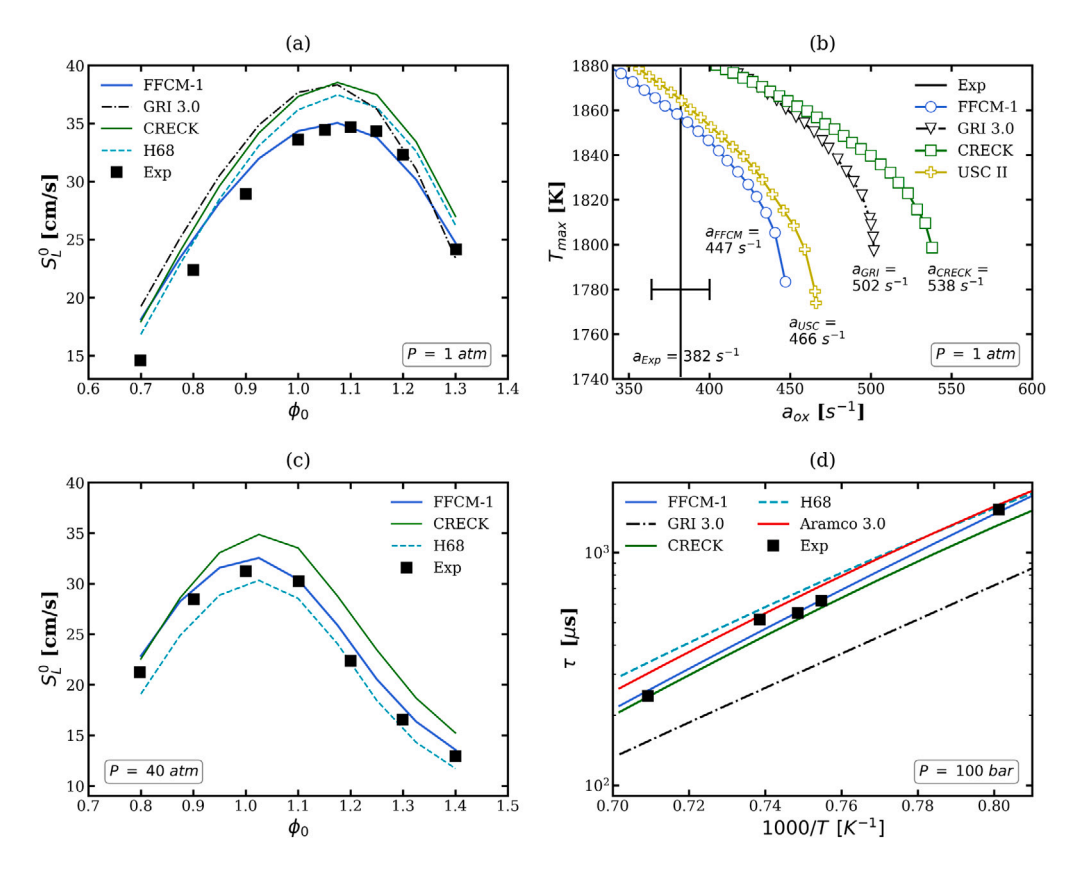


Fig. 1. Validation of kinetic models against experimental data: (a) predictions of CH_4 -air laminar flame speed vs. experimental data (square markers) of Lowry et al. [28] at $\phi_0 = 1.0$ and $T_0 = 298$ K, (b) predictions of CH_4 -air diffusion flame extinction vs. experimental data of Chelliah et al. [29], which is shown as a vertical line with 95% confidence interval, (c) predictions of " CH_4 /17% O_2 /83% He" flame speed vs experimental data (square markers) of Rozenchan et al. [30] at $\phi_0 = 1.0$ and $T_0 = 300$ K, (d) ignition delay predictions benchmarked against experimental data (square markers) of Karimi et al. [31] for a mixture of CH_4 / O_2 /Ar=3:6:91 (mole fraction).

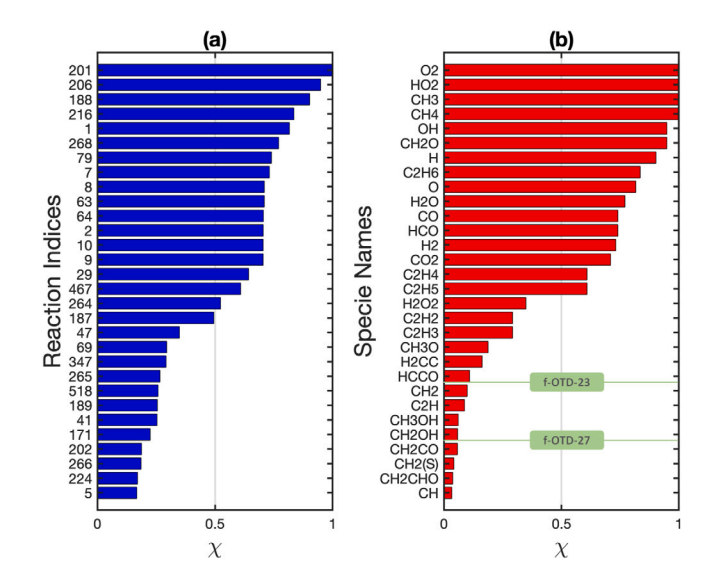


Fig. 2. The FFCM-1 skeletal reduction for methane-air: sorted (a) reactions and (b) species based on their importance as determined by their associated χ values.

ranking the most sensitive species. Several detailed kinetics models are available for methane combustion: GRI 3.0 [35], USC Mech II [36], and CRECK [37] models are usually used for atmospheric pressures (~1 atm), while the foundational fuel chemistry model (FFCM-1) [38], AramcoMech model 3.0 [39], and a model of Hashemi et al. (H68) [40] are utilized for high pressure conditions. Shock tube and/or rapid compression machine experiments are required at high levels of pressure

to gain insight into the underlying kinetics [41-43]. Here, the detailed kinetics model is chosen by benchmarking the predicted laminar flame speeds, the ignition delays, and the extinction curves against experimental data. Figs. 1(a) and 1(c) portray the laminar premixed flame speed predictions by FFCM-1, GRI 3.0, CRECK, and H68. The experimental data at atmospheric and high pressures are taken from Lowry et al. [28] and Rozenchan et al. [30], respectively. It is shown that the flame speeds calculated by FFCM-1 and H68 are in good agreements with the experimental results. Fig. 1(b) shows that the FFCM-1 prediction for diffusion flame extinction is closer to the experimental data of Chelliah and co-workers [29] at 1 atm. Fig. 1(d) benchmarks the ignition delays as predicted by several detailed models against the experimental data of Karimi et al. [31] at 100 bar. Aramco 3.0, CRECK, and FFCM-1 indicate great performances in predicting ignition delays. Based on these comparisons, the FFCM-1 with 38 species and 569 irreversible reactions is selected as the starting bench-marked detailed kinetics model.

2. F-OTD for skeletal reduction

2.1. Reduced-order modeling of the sensitivity with f-OTD

The temporal changes in mass fractions $\psi = [\psi_1, \psi_2, \dots, \psi_{n_s}]^T$ of chemical species and temperature T in an adiabatic, constant pressure P, and spatially homogeneous chemical system of n_s species reacting through n_r irreversible reactions are governed by the following initial value problem [10,44]:

$$\frac{d\xi_{i}}{dt} = f_{i}(\xi, \alpha), \quad \xi(0) = [\psi_{0}, T_{0}], \tag{1}$$

where $\xi = [\psi, T] \in \mathbb{R}^{n_{eq}}$, $f = [f_{\psi}, f_T]$, t is time, and $n_{eq} = n_s + 1$. In Eq. (1), $\alpha = [1, 1, \dots, 1] \in \mathbb{R}^{n_r}$ denotes the vector of

Y. Liu et al. Fuel 357 (2024) 129581

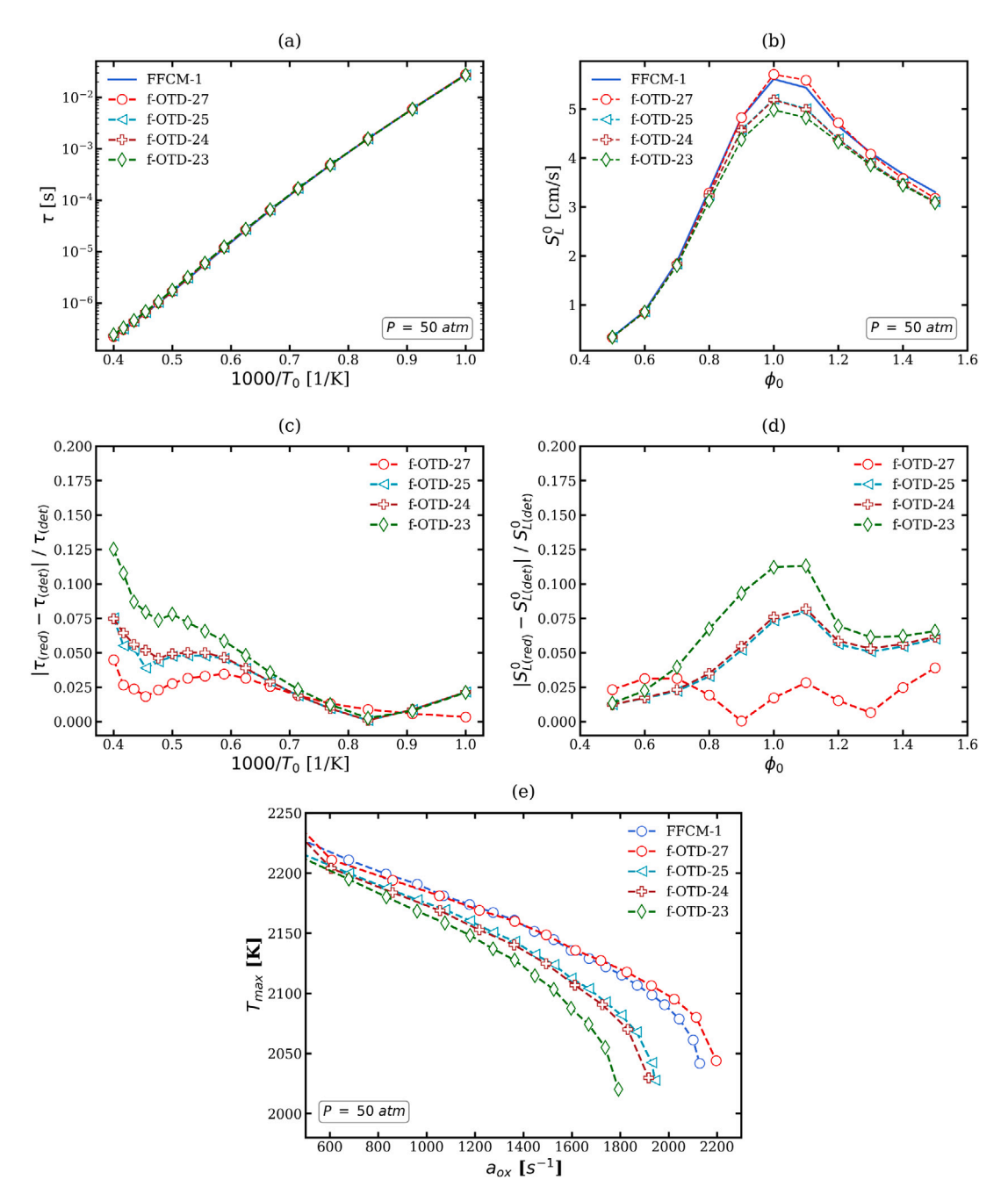


Fig. 3. Predictions via f-OTD skeletal models at P = 50 atm: (a) ignition delays, $\phi_0 = 1.0$, (b) flame speeds, $T_0 = 300$ K, (c) relative errors of skeletal models in terms of the ignition delays, (d) relative errors of skeletal models in terms of the flame speeds, (e) nonpremixed flame extinction with $T_0 = 300$ K.

sensitivity parameters perturbing the progress rate of reactions $Q_j = \alpha_j \mathcal{K}_j \prod_{m=1}^{n_s} (\rho \psi_m / W_m)^{\sqrt{m_j}}$ with $j=1,2,\ldots,n_r$. Here, ρ denotes the density, ν'_{mj} is the molar stoichiometric coefficients of species m in reaction j, and W_m is the molecular weight of species m. A perturbation with respect to α_j around $\alpha_j = 1$, implies an infinitesimal perturbation of Q_j . The parameter \mathcal{K}_j is the forward rate constant of reaction j, which is calculated via the modified Arrhenius model for elementary reactions [45]. All reversible reactions are cast as irreversible reactions. The matrix, $S(t) \in \mathbb{R}^{n_{eq} \times n_r}$, contains local sensitivity coefficients, $S_{ij} = \partial \xi_i / \partial \alpha_i$, and is evolved by solving the sensitivity equation:

$$\frac{dS_{ij}}{dt} = \sum_{m=1}^{n_{eq}} \frac{\partial f_i}{\partial \xi_m} \frac{\partial \xi_m}{\partial \alpha_j} + \frac{\partial f_i}{\partial \alpha_j} = \sum_{m=1}^{n_{eq}} L_{im} S_{mj} + F_{ij}, \tag{2}$$

where $L_{im}=\frac{\partial f_i}{\partial \xi_m}$ and $F_{ij}=\frac{\partial f_i}{\partial \alpha_j}$ denote the Jacobian and the forcing matrices, respectively.

In f-OTD, the sensitivity matrix S(t) is factorized into a time-dependent subspace in the n_{eq} -dimensional phase space of compositions represented by a set of f-OTD modes: $U(t) = [u_1(t), u_2(t), \dots, u_r(t)] \in \mathbb{R}^{n_{eq} \times r}$. These modes are orthonormal: $u_i^T(t)u_j(t) = \delta_{ij}$, where δ_{ij} denotes the Kronecker delta function. The rank of $S(t) \in \mathbb{R}^{n_{eq} \times n_r}$ is $d = \min\{n_{eq}, n_r\}$, while the f-OTD modes represent a rank-r subspace, where $r \ll d$. The sensitivity matrix is approximated via the f-OTD decomposition, $S(t) \approx U(t)Y^T(t)$, where $Y(t) = [\mathbf{y}_1(t), \mathbf{y}_2(t), \dots, \mathbf{y}_r(t)] \in \mathbb{R}^{n_r \times r}$ is the f-OTD coefficient matrix. Therefore, each sensitivity coefficient S_{ij} can be approximated as a finite sum of time-dependent terms: $S_{ij}(t) \approx \sum_{k=1}^r U_{ik}(t)Y_{jk}(t)$. The key characteristic of the model is that both U(t) and Y(t) are time-dependent, and evolve according to the closed form evolution equations extracted from the governing equations of the

Y. Liu et al. Fuel 357 (2024) 129581

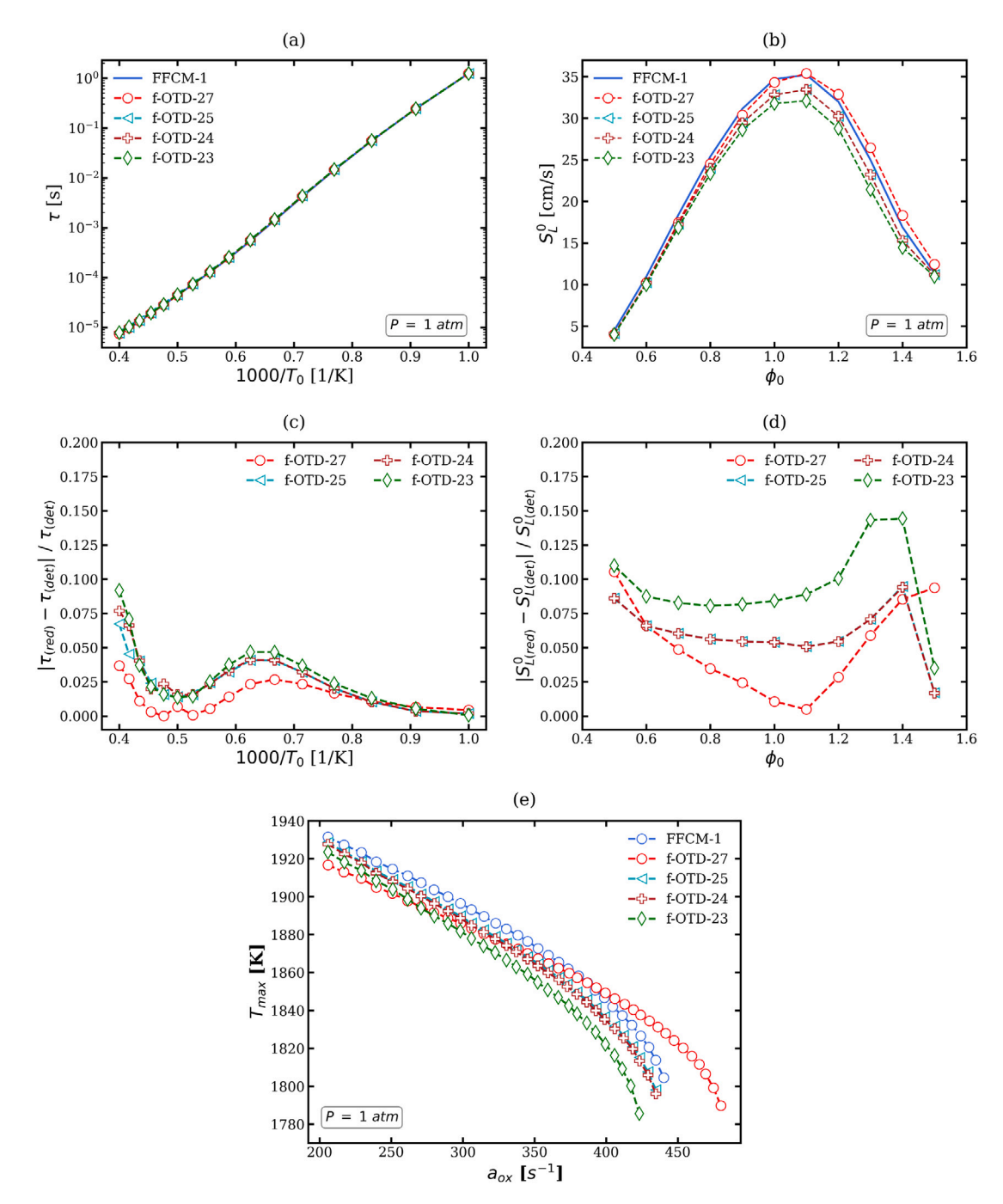


Fig. 4. Predictions via f-OTD skeletal models at P = 1 atm: (a) the ignition delays, $\phi_0 = 1.0$, (b) the flame speeds, $T_0 = 300$ K, (c) relative errors of skeletal models in terms of ignition delays, (d) relative errors of skeletal models in terms of the flame speeds, (e) nonpremixed flame extinction, $T_0 = 300$ K.

system [10]:

$$\frac{dU}{dt} = QLU + QFYC^{-1},\tag{3a}$$

$$\frac{dU}{dt} = QLU + QFYC^{-1},$$
 (3a)
$$\frac{dY}{dt} = YL_r^T + F^TU,$$
 (3b)

where $L_r = U^T L U \in \mathbb{R}^{r \times r}$ is a reduced linearized operator, $Q = I - U U^T$ is the orthogonal projection onto the space spanned by the complement of U, and $C = Y^T Y \in \mathbb{R}^{r \times r}$ is a correlation matrix. The model constructed in this way is able to capture sudden transitions associated with the largest finite time Lyapunov exponents [46,47]. Eq. (3) is a coupled system of ODEs and constitutes the f-OTD evolution equations. The matrix

C(t) is, generally full, implying that the f-OTD coefficients are correlated. The f-OTD modes can become uncorrelated and energetically ranked by rotating the modes along the eigen-direction of the matrix C. When the energy of some of the f-OTD modes are dominant and their singular values are orders of magnitude larger than the energy associated with the other modes, it would be better to use the rank-adaptive and sparse-sampling f-OTD methodology [48,49]. This would circumvent numerical instabilities due to the presence of C^{-1} in Eq. (3a). The f-OTD modes align themselves with the most instantaneously sensitive directions of the composition evolution equation when perturbed by α . These directions can be unambiguously defined as the rank-r reduction of instantaneous singular value decomposition (SVD) of S(t). It has been shown that f-OTD closely approximates the instantaneous SVD of S(t),

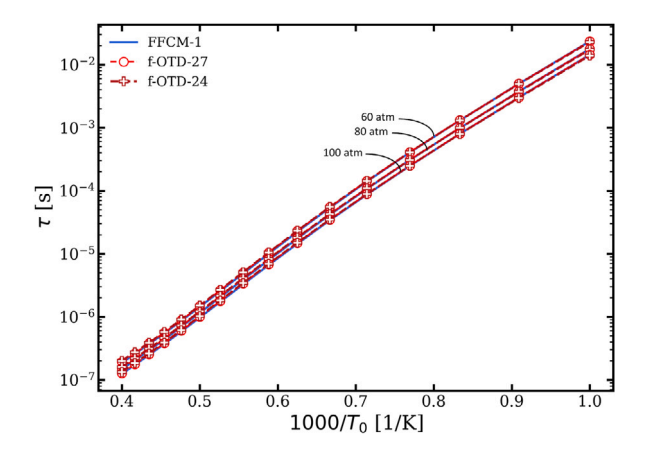


Fig. 5. Predictions via f-OTD-24 and f-OTD-27: Ignition delays for P=60,80, and 100 atm with $\phi_0=1.0.$

and also approximates sensitive directions without having access to any data on full-dimensional S(t) [10]. Similar methodologies via time-dependent bases have also been utilized in stochastic ROM [33,50–53], flow control [54], rare events predictions [55], and ROM of transport equations [56,57].

2.2. Important reactions & species

In f-OTD, modeled sensitivities are computed in factorized format by solving Eqs. (3), in addition to Eq. (1), and the values of ξ , U, and Y are stored at resolved time steps $t_i \in [0, t_f]$. At each resolved time step, and for each case, the eigen decomposition of $S^TS \in \mathbb{R}^{n_r \times n_r}$ as $S^TS = A\Lambda A^T$ are computed along with $\mathbf{w} \in \mathbb{R}^{n_r \times 1} = (\Sigma \lambda_i |a_i|)/(\Sigma \lambda_i) \in \mathbb{R}^{n_r}$. The \mathbf{w} vectors are basically the average of eigenvectors of S^TS matrix weighted based on their associated eigenvalues. This prevents the f-OTD method from dealing with each eigenvector (a_i) separately. The first sorted eigenvalue (λ_1) is usually orders of magnitude larger than the others, which implies $\mathbf{w}(t) \approx |a_1(t)|$. Each element of \mathbf{w} , i.e. w_i , is positive and associated with a certain reaction (ith reaction). The larger the w_i value, the more important the reaction i is. The variable χ_i is used to define as the highest value associated with w_i , i.e. $\chi_i = \max_t(w_i(t))$.

The elements of χ vector are sorted in descending order to find the indices of the most important reactions in the detailed model. Species are also sorted based on their first presence in the sorted reactions, *i.e.* the species which first shows up in a higher ranked reaction are more important than a species that first participate in a lower ranked reaction. This yields in a reaction and species ranking based on the χ vector. Finally, a set of species are chosen by setting the threshold χ_{ϵ} on the element of χ vector and eliminating species whose associated χ_i values are smaller. The skeletal model reduction is reaction based, thus any non-reactive species with non-zero mass fraction in the initial condition should be manually added to the skeletal model, such as N_2 and/or Ar.

In summary, the f-OTD method instantaneously observes the ignition system, and sorts the reactions based on their effects on sensitivities to find the most important species. These species and the reactions which connect them together create the skeletal models. In chemical kinetic systems, perturbations with respect to "fast" reactions generate very large sensitivities for short time periods, but these sensitivities vanish as $t \to \infty$. On the other hand, perturbations with respect to "slow" reactions generate smaller and more sustained sensitivities. Since the approach is based on the instantaneous observation of sensitivities, both slow and fast reactions can leave an imprint on the instantaneous normalized reaction vector (\boldsymbol{w}) . However, if the sensitivities associated with these reactions would be averaged together over

Table 1

FFCM-1 based skeletal models.

Model	n_s	n_r	χ_{ϵ}
FFCM-1	38	569	0
f-OTD-27	27	319	0.0583
f-OTD-25	25	261	0.0877
f-OTD-24	24	247	0.0992
f-OTD-23	23	213	0.1093

a period of time, then the smaller sensitivities associated with slow reactions could be out-weighted by the large sensitivities associated with fast reactions.

3. Skeletal reduction of FFCM-1

The f-OTD method is employed to compute local sensitivities based on Eq. (3) for atmospheric and high pressure ignition of methane. The U and Y matrices are initialized by solving the sensitivity equation (Eq. (2)) for few time steps, and then performing singular value decomposition on the sensitivity matrix. All f-OTD simulations are performed with r=2. The initial conditions for temperature, pressure, and equivalence ratio are $T_0 \in \{1200, 1500, 2000\}$ K, $P \in \{1, 20, 40, 60, 80, 100\}$ atm, and $\phi \in \{0.5, 1.0, 1.5\}$, respectively. Therefore, in total 48 cases are considered. As described in §2, the outcome of the reduction process is a series of skeletal models as listed in Table 1. The generated f-OTD models are labeled by "f-OTD-X" in which "X" denotes the number of species included in the model. In Table 1, n_r shows the number of irreversible reactions in each of the models.

3.1. Reactions and species ranking

Fig. 2 shows the species and reaction rankings based on the process described in Section 2.2. Reactions R201 ($O_2 + CH_4 \rightarrow CH_3 + HO_2$), R206 ($CH_3 + O_2 \rightarrow OH + CH_2O$), and R188 (CH_4 (+M) $\rightarrow CH_3 + H$ (+M)) are identified as the top three most important ones in FFCM-1 for methane ignition. The oxidation of methane is initiated by its reaction with molecular oxygen (R201). The methyl radical (CH_3) then reacts with the molecular oxygen to form $OH + CH_2O$ via R206. As for the species, O_2 , HO_2 , CH_3 , CH_4 , OH, CH_2O , OH_2O , OH_2O are the top 10 most important ones. The f-OTD-23 model contains the top 22 ranked species in Fig. 2(b) plus nitrogen (non-reactive species with non-zero initial mass fractions). The f-OTD-24, f-OTD-25, f-OTD-26, and f-OTD-27 models are produced by adding, respectively, CH_2 , C_2H , CH_3OH , and CH_2OH and their reactions step by step to f-OTD-23.

3.2. Skeletal model validation

The performances of the reduced models are assessed by comparing their estimations for the ignition delays, the laminar flame speeds, and the counter-flow extinction strains against FFCM-1 for different mixtures. Here, the ignition delay is defined as the time required by carbon monoxide (CO) to reach its maximum production rate. The flame speeds and the extinction curves are generated by Cantera [58] with a plug flow boundary condition assumption [59] for extinction simulations.

Fig. 3 compares the f-OTD results at P=50 atm against FFCM-1. Fig. 3(a) and (c) show that f-OTD models with $n_s \geq 24$ predict ignition delays with less than 10% error for $T_0 \in [1000, 2500]$ K, and less than 5% error for $T_0 \in [1000, 1670]$ K. The f-OTD-27 is the most accurate skeletal model for estimating ignition delays at P=50 atm with less than 5% overall error. Fig. 3(b) and (d) portray the ability of f-OTD-24, f-OTD-25, and f-OTD-27 models in reproducing the laminar flame speeds of FFCM-1 with less than 10% error. The maximum error of f-OTD-27 for flame speed estimations is 3%. Fig. 3(e) shows that the f-OTD model with 27 species reproduces the extinction curve of FFCM-1

Y. Liu et al. Fuel 357 (2024) 129581

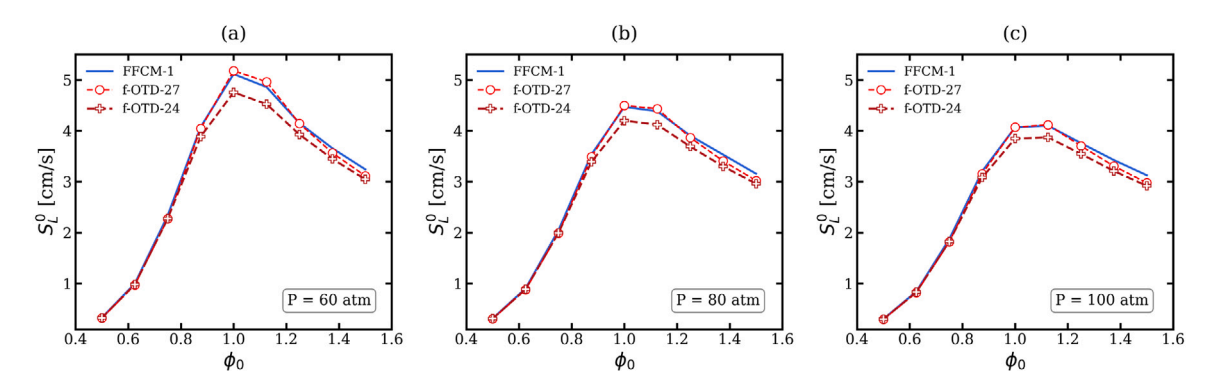


Fig. 6. Predictions via f-OTD-24 and f-OTD-27: Laminar flame speeds for P = 60,80, and 100 atm with $T_0 = 300\,$ K.

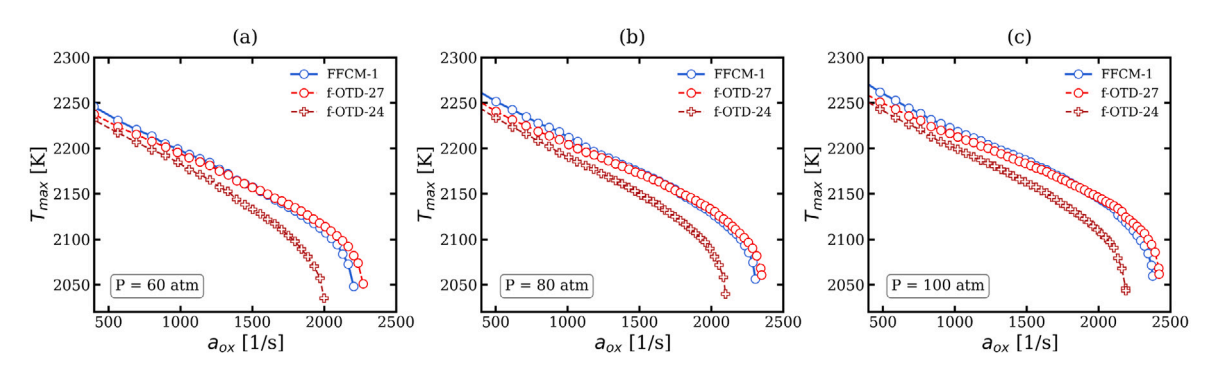


Fig. 7. Predictions via f-OTD-24 and f-OTD-27: Diffusion flame extinction for P = 60, 80, and 100 atm with $T_0 = 300$ K.

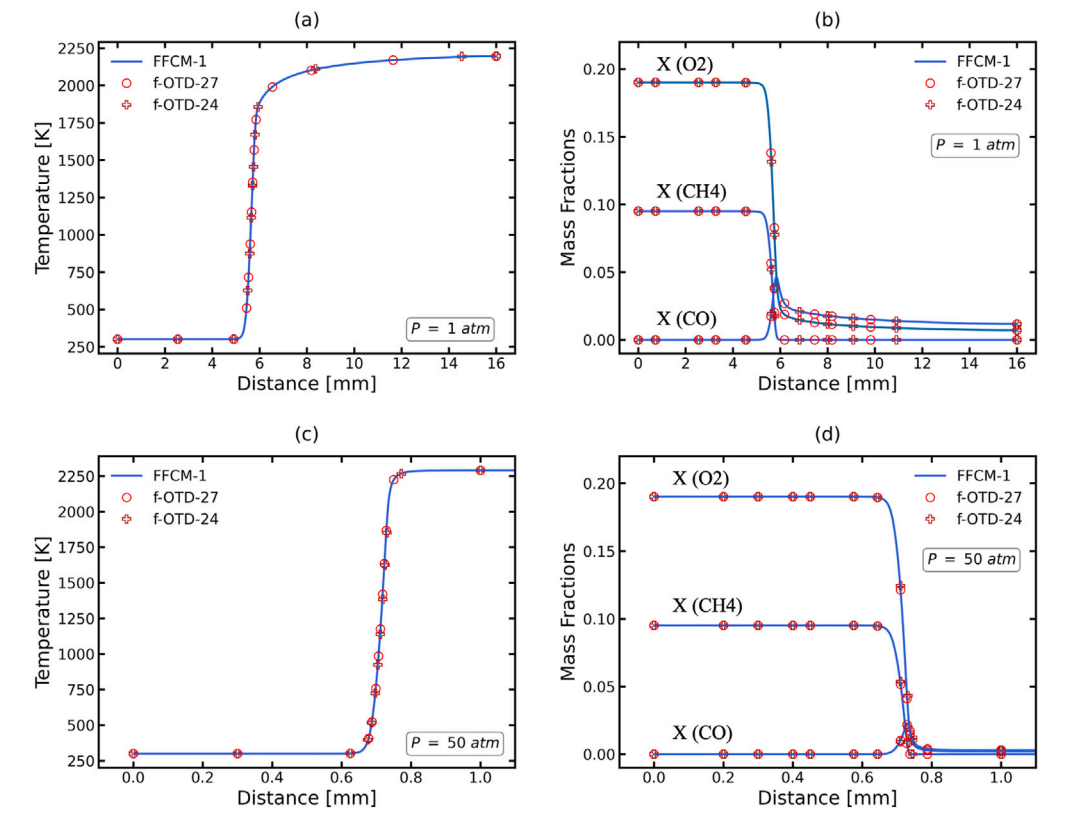


Fig. 8. Prediction via f-OTD-24 and f-OTD-27: 1 D freely-propagating, premixed flame structure with $T_0 = 300$ K, $\phi_0 = 1.0$, and P = 1&50 atm.

almost exactly. Altogether, the accuracy of f-OTD models in regenerating FFCM-1 results improves with increasing the number of species. Moreover, f-OTD-24 and f-OTD-25 show very similar predictions. This means that while $\rm C_2H$ is an important species, including it in f-OTD-25 does not change the predictions significantly.

Fig. 4 shows the performance of f-OTD models at P=1 atm. Figs. 4(a), (b), (c), and (d) indicate better performances of the models in predicting the ignition delays and the laminar flame speeds by increasing n_s . The f-OTD-27 is the most accurate model with less than 5% error in estimating ignition delays, and 10% error in predicting laminar flame speeds. However, the flame speeds calculated by f-OTD-27 have larger errors for very lean and very rich fuels, *i.e.* $\phi_0 < 0.6$ and $\phi_0 > 1.4$. Altogether, Fig. 4 suggests that at atmospheric pressure, f-OTD model with $n_s \ge 24$ provides reasonable predictions for the three quantities as considered.

Figs. 5–7 demonstrate the ability of f-OTD-24 and f-OTD-27 in reproducing the FFCM-1 results, over a wide range of pressures (P=60 atm, 80 atm, and 100 atm). Fig. 5 compares the ignition delays predicted by these f-OTD models against FFCM-1, and Fig. 6 indicates that f-OTD-24 and f-OTD-27 estimate the FFCM-1 flame speeds accurately. The f-OTD-27 predicts the laminar flame speeds reasonably well, with its worst predictions at $\phi_0 > 1.2$ where the relative error is still less than 10%. Fig. 6 also shows that the maximum flame speed decreases by increasing the pressure from 60 atm to 100 atm. Fig. 7 compares the extinction curves of f-OTD-24 and f-OTD-27 against FFCM-1. Both models perform very well in this high pressure condition. Fig. 8 shows the structure of freely-propagating, premixed flame of methane at two different pressures, *i.e.* P=1 atm and P=50 atm. f-OTD-24 and f-OTD-27 reproduce the temperature and mass fractions predictions of FFCM-1 with a good accuracy.

4. Conclusions

New skeletal kinetics models are generated from the FFCM-1 for the methane combustion at atmospheric and high pressure conditions. In the reduction process, local sensitivities are computed by the f-OTD method for the auto-ignition problem with different sets of initial conditions. The calculated sensitivities are then analyzed, and the 38 species of the FFCM-1 are ranked based on their importance. Different skeletal models with different levels of accuracy are generated by selecting more high ranked species. The ignition delays, the laminar flame speeds, and the diffusion flame extinctions predicted by the generated models are benchmarked against FFCM-1. The results show the model with 27 species and 319 irreversible reactions accurately reproduces the predictions of FFCM-1 at all conditions. The model with 24 species and 247 irreversible reactions also provides reasonable predictions. Therefore, f-OTD-24 and f-OTD-27 are the recommended skeletal models for the FFCM-1 over the observed range of pressures, temperatures, and equivalence ratios. The Cantera format (.cti) of these skeletal models are supplied in Appendix.

The f-OTD method has demonstrated its ability for reduced order modeling of local sensitivities in time dependent combustion systems, and is recommended for future multi-dimensional reacting flow simulations. The described local sensitivity analysis technique for skeletal reduction is also recommended for other detailed kinetics models. This technique does not require a priori expert knowledge of chemistry, thus can be used for skeletal reduction of very large reaction networks, e.g. heavy hydrocarbon fuels like JP-10 (C $_{10}H_{16}$). For future work the f-OTD method is recommended for skeletal reduction of very large reaction networks, i.e. with $\mathcal{O}(1000)$ species, by implementing rank-adaptive and sparse-sampling techniques [48,49].

CRediT authorship contribution statement

Yinmin Liu: Investigation. Hessam Babaee: Investigation. Peyman Givi: Investigation. Harsha K. Chelliah: Investigation. Daniel Livescu: Investigation. Arash G. Nouri: Investigation.

Declaration of competing interest

The authors declare the following financial interests/personal relationships which may be considered as potential competing interests: Peyman Givi reports financial support was provided by Los Alamos National Laboratory. Peyman Givi reports financial support was provided by National Science Foundation.

Data availability

Data will be made available on request.

Acknowledgments

This work has been co-authored by an employee of Triad National Security, LLC which operates Los Alamos National Laboratory under Contract No. 89233218CNA000001 with the U.S. Department of Energy/National Nuclear Security Administration. The work at Pitt is sponsored by the National Science Foundation (NSF) under Grant CBET-2042918 and Grant CBET-2152803. Computational resources are provided by the Center for Research Computing (CRC) at Pitt.

Appendix

All reduced mechanisms developed in this work can be accessed via this link.

References

- Kohse Höinghaus K. Combustion in the future: The importance of chemistry. Proc Combust Inst 2021;38(1):1–56.
- [2] Gorban AN. Model reduction in chemical dynamics: Slow invariant manifolds, singular perturbations, thermodynamic estimates, and analysis of reaction graph. Curr Opin Chem Eng 2018;21:48–59.
- [3] Lu T, Law C. Toward accommodating realistic fuel chemistry in large-scale computations. Prog Energy Combust Sci 2009;35(2):192–215.
- [4] Goussis D, Maas U. Model reduction for combustion chemistry. In: Turbulent combustion modeling. Springer; 2011, p. 193–220.
- [5] Smooke MD. Reduced kinetic mechanisms and asymptotic approximations for methane-air flames: A topical volume. Springer; 1991.
- [6] Peters N, Rogg B. Reduced kinetic mechanisms for applications in combustion systems. Vol. 15 of lecture notes in physics, Berlin, Germany: Springer-Verlag; 1993
- [7] Turányi T. Sensitivity analysis of complex kinetic systems, tools and applications. J Math Chem 1990;5(3):203–48.
- [8] Tomlin AS. The role of sensitivity and uncertainty analysis in combustion modelling. Proc Combust Inst 2013;34(1):159–76.
- [9] vom Lehn F, Cai L, Pitsch H. Sensitivity analysis, uncertainty quantification, and optimization for thermochemical properties in chemical kinetic combustion models. Proc Combust Inst 2019;37(1):771–9.
- [10] Nouri A, Babaee H, Givi P, Chelliah H, Livescu D. Skeletal model reduction with forced optimally time dependent modes. Combust Flame 2022;235:111684.
- [11] Lam S, Goussis D. The CSP method for simplifying kinetics. Int J Chem Kinet 1994;26(4):461–86.
- [12] Neophytou M, Goussis D, Van Loon M, Mastorakos E. Reduced chemical mechanisms for atmospheric pollution using computational singular perturbation analysis. Atmos Environ 2004;38(22):3661–73.
- [13] Lu T, Law CK. A criterion based on computational singular perturbation for the identification of quasi steady state species: A reduced mechanism for methane oxidation with no chemistry. Combust Flame 2008;154(4):761–74.
- [14] Turanyi T. Reduction of large reaction mechanisms. New J Chem 1990;14(11):795–803.
- [15] Wang H, Frenklach M. Detailed reduction of reaction mechanisms for flame modeling. Combust Flame 1991;87(3-4):365-70.
- [16] Sun W, Chen Z, Gou X, Ju Y. A path flux analysis method for the reduction of detailed chemical kinetic mechanisms. Combust Flame 2010;157(7):1298–307.
- [17] Lu T, Law CK. A directed relation graph method for mechanism reduction. Proc Combust Inst 2005;30(1):1333–41.
- [18] Pepiot-Desjardins P, Pitsch H. An efficient error-propagation-based reduction method for large chemical kinetic mechanisms. Combust Flame 2008;154(1–2):67–81.
- [19] Niemeyer KE, Sung C-J, Raju MP. Skeletal mechanism generation for surrogate fuels using directed relation graph with error propagation and sensitivity analysis. Combust Flame 2010;157(9):1760–70.

- [20] Brown N, Li G, Koszykowski M. Mechanism reduction via principal component analysis. Int J Chem Kinet 1997;29(6):393–414.
- [21] Esposito G, Chelliah H. Skeletal reaction models based on principal component analysis: Application to ethylene–air ignition, propagation, and extinction phenomena. Combust Flame 2011;158(3):477–89.
- [22] Parente A, Sutherland J, Dally B, Tognotti L, Smith P. Investigation of the MILD combustion regime via principal component analysis. Proc Combust Inst 2011;33(2):3333-41.
- [23] Parente A, Sutherland J. Principal component analysis of turbulent combustion data: Data pre-processing and manifold sensitivity. Combust Flame
- [24] Mirgolbabaei H, Echekki T. Nonlinear reduction of combustion composition space with kernel principal component analysis. Combust Flame 2014;161(1):118–26.
- [25] Coussement A, Isaac B, Gicquel O, Parente A. Assessment of different chemistry reduction methods based on principal component analysis: Comparison of the MG-PCA and score-PCA approaches. Combust Flame 2016;168:83–97.
- [26] Malik M, Isaac B, Coussement A, Smith P, Parente A. Principal component analysis coupled with nonlinear regression for chemistry reduction. Combust Flame 2018;187:30–41.
- [27] Stagni A, Frassoldati A, Cuoci A, Faravelli T, Ranzi E. Skeletal mechanism reduction through species-targeted sensitivity analysis. Combust Flame 2016;163:382–93.
- [28] Lowry W, de Vries J, Krejci M, Petersen E, Serinyel Z, Metcalfe W, et al. Laminar flame speed measurements and modeling of pure alkanes and alkane blends at elevated pressures. J Eng Gas Turbine Power 2011;133(9).
- [29] Sarnacki B, Esposito G, Krauss R, Chelliah H. Extinction limits and associated uncertainties of nonpremixed counterflow flames of methane, ethylene, propylene and n-butane in air. Combust Flame 2012;159(3):1026–43.
- [30] Rozenchan G, Zhu DL, Law CK, Tse SD. Outward propagation, burning velocities, and chemical effects of methane flames up to 60 atm. Proc Combust Inst 2002;29(2):1461–70.
- [31] Karimi M, Ochs B, Liu Z, Ranjan D, Sun W. Measurement of methane autoignition delays in carbon dioxide and argon diluents at high pressure conditions. Combust Flame 2019:204:304–19.
- [32] Donello M, Carpenter MH, Babaee H. Computing sensitivities in evolutionary systems: A real-time reduced order modeling strategy. SIAM J Sci Comput 2022;A128–49.
- [33] Patil P, Babaee H. Real-time reduced-order modeling of stochastic partial differential equations via time-dependent subspaces. J Comput Phys 2020;415:109511.
- [34] Koch O, Lubich C. Dynamical low-rank approximation. SIAM J Matrix Anal Appl 2007;29(2):434–54.
- [35] Smith GP, Golden DM, Frenklach M, Moriarty NW, Eiteneer B, Goldenberg M, et al. Gri-Mech 3.0, http://www.me.berkeley.edu/gri_mech/.
- [36] Wang H, You X, Joshi AV, Davis SG, Laskin A, Egolfopoulos F, et al. [U]sc Mech Version ii. High-temperature Combustion Reaction Model of h2/co/c1-c4 Compounds. http://ignis.usc.edu/USC.Mech II.htm.
- [37] Ranzi E, Frassoldati A, Grana R, Cuoci A, Faravelli T, Kelley A, et al. Hierarchical and comparative kinetic modeling of laminar flame speeds of hydrocarbon and oxygenated fuels. Prog Energy Combust Sci 2012;38(4):468–501.
- [38] Smith G, Tao Y, Wang H. Foundational fuel chemistry model version 1.0 (ffcm-1). 2016, http://nanoenergy.stanford.edu/ffcm1.
- [39] Zhou CW, Li Y, Burke U, Banyon C, Somers KP, Ding S, et al. An experimental and chemical kinetic modeling study of 1, 3-butadiene combustion: Ignition delay time and laminar flame speed measurements. Combust Flame 2018;197:423–38.

- [40] Hashemi H, Christensen JM, Gersen S, Levinsky H, Klippenstein SJ, Glarborg P. High-pressure oxidation of methane. Combust Flame 2016;172:349–64.
- [41] Pierro M, Laich A, Urso JJ, Kinney C, Vasu S, Albright MA. Ignition delay times of methane fuels at thrust chamber conditions in an ultra-high-pressure shock tube. In: AIAA SCITECH 2022 forum. 2022, p. 1254.
- [42] Shao J, Ferris AM, Choudhary R, Cassady SJ, Davidson DF, Hanson RK. Shock-induced ignition and pyrolysis of high-pressure methane and natural gas mixtures. Combust Flame 2020;221:364–70.
- [43] Li Y, Zhou CW, Somers KP, Zhang K, Curran HJ. The oxidation of 2-butene: A high pressure ignition delay, kinetic modeling study and reactivity comparison with isobutene and 1-butene. Proc Combust Inst 2017;36(1):403–11.
- [44] Zsely I, Zador J, Turanyi T. Similarity of sensitivity functions of reaction kinetic models. J Phys Chem A 2003;107(13):2216–38.
- [45] Williams FA. Combustion theory. second ed.. London: CRC Press, Taylor Francis Group; 1985.
- [46] Babaee H, Sapsis T. A minimization principle for the description of modes associated with finite-time instabilities. Proc R Soc Lond Ser A Math Phys Eng Sci 2016;472(2186):20150779.
- [47] Babaee H, Farazmand M, Haller G, Sapsis T. Reduced-order description of transient instabilities and computation of finite-time Lyapunov exponents. Chaos 2017;27(6):063103.
- [48] Donello M, Palkar G, Naderi MH, Del Rey Fernández DC, Babaee H. CUR decomposition for scalable rank-adaptive reduced-order modeling of nonlinear stochastic PDEs with time-dependent bases. 2023, arXiv:2305.04291.
- [49] Naderi MH, Babaee H. Adaptive sparse interpolation for accelerating nonlinear stochastic reduced-order modeling with time-dependent bases. Comput Methods Appl Mech Engrg 2023;405:115813.
- [50] Sapsis T, Lermusiaux P. Dynamically orthogonal field equations for continuous stochastic dynamical systems. Phys D: Nonlinear Phenom 2009;238(23–24):2347–60.
- [51] Cheng M, Hou T, Zhang Z. A dynamically bi-orthogonal method for time-dependent stochastic partial differential equations i: Derivation and algorithms. J Comput Phys 2013;242:843–68.
- [52] Babaee H, Choi M, Sapsis TP, Karniadaki GE. A robust biorthogonal/dynamically-orthogonal method using the covariance pseudo-inverse with application to stochastic flow problems. J Comput Phys 2017;344:303–19.
- [53] Babaee H. An observation-driven time-dependent basis for a reduced description of transient stochastic systems. Proc R Soc A: Math Phys Eng Sci 2019;475(2231):20190506.
- [54] Blanchard A, Mowlavi S, Sapsis T. Control of linear instabilities by dynamically consistent order reduction on optimally time-dependent modes. Nonlinear Dynam 2019;95(4):2745–64.
- [55] Farazmand M, Sapsis T. Dynamical indicators for the prediction of bursting phenomena in high-dimensional systems. Phys Rev E 2016;94:032212.
- [56] Ramezanian D, Nouri A, Babaee H. On-the-fly reduced order modeling of passive and reactive species via time-dependent manifolds. Comput Methods Appl Mech Engrg 2021;382:113882.
- [57] Amiri-Margavi A, Babaee H. On-the-fly reduced-order modeling of transient flow response subject to high-dimensional external forcing. Indianapolis, IN: American Physical Society Division of Fluid Dynamics; 2022.
- [58] Goodwin D, Moffat H, Speth R. Cantera: An object-oriented software toolkit for chemical kinetics, thermodynamics, and transport processes. 2017, http://www.cantera.org, Version 2.6.0.
- [59] Fiala T, Sattelmayer T. Nonpremixed counterflow flames: Scaling rules for batch simulations. J Combust 2014.